THE JOURNAL OF IMMUNOLOGY

Coupled IL-2–Dependent Extracellular Feedbacks Govern Two Distinct Consecutive Phases of CD4 T Cell Activation

Nir Waysbort, Dor Russ, Benjamin M. Chain and Nir Friedman

J Immunol 2013; 191:5822-5830; Prepublished online 15 November 2013;
doi: 10.4049/jimmunol.1301575
http://www.jimmunol.org/content/191/12/5822

The Journal of Immunology is published twice each month by
The American Association of Immunologists, Inc.,
9650 Rockville Pike, Bethesda, MD 20814-3994.

Print ISSN: 0022-1767 Online ISSN: 1550-6606.

Coupled IL-2–Dependent Extracellular Feedbacks Govern Two Distinct Consecutive Phases of CD4 T Cell Activation

Nir Waysbort,* Dor Russ,* Benjamin M. Chain,[†,1] and Nir Friedman*,[1]

T cells integrate cell-specific Ag receptor signaling with shared signals mediated by secreted cytokines, which often involve regulatory feedback loops. IL-2 signaling, for example, reduces the synthesis of IL-2 and increases the synthesis of IL-2Rα-chain, whereas both genes require TCR signaling for their activation. The ways by which T cells dynamically integrate these private and public signals during activation are not well understood. We combined robotics, multiparameter flow cytometry, and real-time quantitative PCR to analyze T cell activation at high temporal resolution over several days. Two distinct temporal phases of T cell activation were evident. First, Ag-dependent signals activated low IL-2Rα and high IL-2 production, independent of IL-2 signaling. Subsequently, secreted IL-2 acted as a shared resource driving high IL-2Rα expression, reduced IL-2 synthesis, and cell proliferation. This transition was independent of continued TCR signaling. Our data allowed the determination of the parameters of the IL-2–mediated extracellular positive and negative feedback circuits and demonstrated that the two loops are coupled and become activated at a similar level of IL-2 signaling. We propose that temporal separation of private and shared signals allows T cells to first integrate Ag-specific responses and subsequently share information leading to collective decision making. ***The Journal of Immunology*****, 2013, 191: 5822–5830.**

Naive CD4 T cell activation is controlled by Ag binding to the TCR in concert with a host of additional inputs from the APC and the microenvironment. These nonspecific inputs can be further classified as signals that are restricted to an individual cell–cell interaction (e.g., costimulatory interactions at the immunological synapse) and those which can be shared between several neighboring cells, such as those mediated by secreted cytokines. We denote the former as private signals and the latter as public. Of note, many of these cytokines can be secreted by activated T cells themselves, resulting in multiple intercellular autocrine and paracrine feedbacks. These feedback loops interact in a variety of complex nonlinear ways. Of particular interest is to establish the interplay between the private and public inputs. The system also operates in several different timescales (1–3); signaling events proximal to receptor binding are typically rapid [seconds to minutes (4)], but cytokine production takes hours, and proliferation requires days. The delay in output is likely to be important to allow different signals to integrate, hence, facilitating more complex decision processes to be implemented. The ways by which T cells dynamically integrate information from different signaling pathways at different timescales during activation are still poorly understood.

One of the most extensively studied aspects of T cell activation has been the role of IL-2 and the IL-2R complex. IL-2 was originally described as a cytokine responsible for driving effector and memory T cell proliferation (5). Paradoxically, however, IL-2–deficient mice were found to develop autoimmune syndromes (6), a phenomenon later attributed to the role of IL-2 in the generation, expansion, and maintenance of regulatory T (Treg) cells (7, 8). IL-2 is secreted by T cells upon TCR activation and exerts its major physiological roles via the IL-2R, a complex of three chains, α, β, and γ, which together form the high-affinity receptor unit (9). Recently, a quantitative understanding of the relationship between the concentrations of IL-2 and its receptor's subunits, and the level of downstream signaling was gained (10, 11). IL-2 also drives two extracellular feedback loops that play a key role in the process of T cell activation: a positive feedback loop that enhances IL-2RA expression (12, 13) and a negative feedback loop in which IL-2 signaling inhibits subsequent IL-2 expression (14).

Although IL-2 and TCR signaling have been studied separately at the molecular level, their integration during the process of naive T cell activation is yet to be elucidated. In particular, questions remain regarding the temporal segregation of the two signals, their eventual integration over the longer timeframe and their relative contribution to proliferation. To answer these questions, we used a systems immunology approach to explore the kinetic relationship between the TCR-dependent and IL-2R–dependent events in the process of T cell activation. We used a robotic system to sample cultures of T cells during their activation by APCs at a high temporal resolution of 3 h for up to 4 d. We characterized cell state and proliferation by multiparameter flow cytometry and quantitative real time PCR (RT-qPCR) to analyze the detailed dynamics of T cell response following activation. This high temporal resolution data of mRNA and protein levels in response to different Ag doses and perturbations of TCR and IL-2 signaling allowed us to quantitatively evaluate kinetic parameters of the system and to dissect its dependence on these two signals and their temporal segregation.

*Department of Immunology, Weizmann Institute of Science, Rehovot 76100, Israel; and [†]Division of Infection and Immunity, University College London, London WC1E 6BT, United Kingdom

[1]B.M.C. and N.F. contributed equally to this work.

Received for publication June 26, 2013. Accepted for publication October 14, 2013.

This work was supported by a grant from Weizmann U.K., by the Abisch–Frenkel Foundation, and by the Converging Technologies Program of the Israel Science Foundation (Grant 1752/07). N.F. is incumbent of the Pauline Recanati Career Development Chair of Immunology.

Address correspondence and reprint requests to Dr. Nir Friedman, Department of Immunology, Weizmann Institute of Science, Rehovot 76100, Israel. E-mail address: nir.friedman@weizmann.ac.il

The online version of this article contains supplemental material.

Abbreviations used in this article: CsA, cyclosporin A; DC, dendritic cell; FSC, forward light scatter; KO, knockout; MCC, moth cytochrome c; MFI, mean fluorescence intensity; RT-qPCR, quantitative real-time PCR; Treg, regulatory T.

www.jimmunol.org/cgi/doi/10.4049/jimmunol.1301575

Materials and Methods

Mice and cell culture

5C.C7 TCR transgenic mice and IL2GFP^{ki} mice used in this study were bred and maintained at the Weizmann Institute of Science Animal Facility under specific pathogen-free conditions in accordance with institutional guidelines. IL2GFP^{ki} mice (5C.C7-IL2KO) were provided by H. Gu (Columbia University, New York, NY). C3H/HeSnJ mice were purchased from Harlan Industries (Indianapolis, IN). Splenocytes were extracted from 5C.C7 TCR transgenic mice and IL2GFP^{ki} mice and meshed into single-cell suspension and enriched for naive CD4 T cells using CD4$^+$CD62L$^+$ T Cell Isolation Kit II (Miltenyi Biotec, Bergisch Gladbach, Germany). Splenocytes also were extracted from C3H/HeSnJ mice and treated with collagenase and DNAse (0.1 mg/ml) and then enriched for dendritic cells (DCs) using CD11c MicroBeads (Miltenyi Biotec). T cells were stained with 1.5 μM CFSE, and 10^5 T cells were incubated with 2×10^4 DC and moth cytochrome c (MCC) peptide (ANERADLIAYLKQATK) at different concentrations in standard growing medium (RPMI 1640 medium supplemented with 10% FBS, L-glutamine, sodium pyruvate, nonessential amino acids, penicillin/streptomycin, kanamycin, and β-mercaptoethanol). In some experiments IL-2 was added to the media at a concentration of 100 ng/ml. In other experiments, cyclosporin A (CsA) (Sandimmune, Novartis, NJ) was added to the medium at a concentration of 100 ng/ml either at the start of culture or at 19 h, as indicated.

A robotic system for cell culture and sampling

For high temporal resolution sampling, we used a robotic system for cell culture and sampling (Freedom EVO; Tecan, Männedorf, Switzerland). The system includes a compatible cell incubator, a robotic centrifuge, temperature controlled plate holders, and automated liquid handling. Cell cultures (peptide loaded DCs and T cells, as described above) were grown in 96-well plates in the robotic incubator. Every 3 h, a plate was removed from the incubator, and cells from one well (out of several identical replicate cultures that were started at the same time) were sampled into another plate. Half of the cells were stored at 4°C for further manual Ab staining and analysis as described below. Half of the cells were used for mRNA extraction by the robotic system, followed by RT-qPCR analysis.

Staining and FACS

Cells were harvested at different times post incubation, and stained with allophycocyanin anti–CD25 (PC61; BioLegend, San Diego, CA), PE-anti-CD122 (5H4, TMbeta; BioLegend), and LIVE/DEAD Fixable Blue Dead Cell Stain Kit for UV excitation (Invitrogen, Carlsbad, CA). Cells were read with LSR-II FACS machine (BD Biosciences, Franklin Lakes, NJ) using FACSDiva software and analyzed using MATLAB (MathWorks, Natick, MA).

ImageStreamX

Cells were harvested and stained as for FACS and prepared for reading, according to the manufacturer's instructions. Data were analyzed using IDEAS software (Amnis, Seattle, WA), provided by the manufacturer. To calculate the distribution of CD25 on cells, the built-in Δ Centroid XY function was used, which is the root of the sum of squares of each δ centroid. Forward light scatter (FSC) and CD25 fluorescence channels were used as masks. Cell area was calculated using the Area feature of the IDEAS software.

ELISA

Medium was collected from the wells immediately prior to harvesting, and ELISA was performed using anti–IL-2 Ab clones: JES6-1A12, JES6-5H4 (BioLegend). Standard curves were prepared with the same protein batch used for cell incubation.

mRNA

For RT-qPCR analysis, RNA was extracted using RNeasy Mini Kit (Qiagen, Hilden, Germany), according to the manufacturer's recommendations, and cDNA was prepared using Moloney murine leukemia virus reverse transcriptase (Promega, Madison, WI), according to the manufacturer's recommendations for oligo(dT)15. Gene-specific relative expression levels were quantified by real-time PCR using the AB 7300 Real Time System (Applied Biosystems, Foster City, CA). Amplification was carried out in a total volume of 20 μl using platinum SYBR Green (Invitrogen). Samples were run in triplicate, and their relative expression was determined by normalizing expression of each time point to its cell number and then comparing this normalized value to the normalized $t = 0$. Primers used were the following: IL-2, 5′-CGGCATGTTCTGGATTT-3′ (forward) and 5-AGGTACATAGTTATTGAGGGC-3′ (reverse); and IL-2RA, 5′-TGTGCTCACAATGGAGTATAAGG-3′ (forward) and 5′-CTCAGGAGGAGGATGCTGAT-3′ (reverse).

Extracting the response functions of IL-2 and IL-2RA from high temporal resolution data

To extract the response functions of the two feedback loops governing IL-2RA and IL-2 expression, we used the following set of differential equations that describe the system:

$$\frac{dIL\text{-}2_{mRNA}}{dt} = K_{IL\text{-}2} + f_1(IL\text{-}2_P \cdot IL\text{-}2RA_P) - \alpha_{IL\text{-}2\_mRNA} \cdot IL\text{-}2_{mRNA} \quad (1)$$

$$\frac{dIL\text{-}2RA_{mRNA}}{dt} = K_{IL\text{-}2RA} + f_2(IL\text{-}2_P \cdot IL\text{-}2RA_P) - \alpha_{IL\text{-}2RA\_mRNA} \cdot IL\text{-}2RA_{mRNA} \quad (2)$$

where $IL\text{-}2_{mRNA}$ and $IL\text{-}2RA_{mRNA}$ are the mRNA levels of IL-2 and IL-2RA, respectively; $K_{IL\text{-}2}$ and $K_{IL\text{-}2RA}$ are the IL-2–independent rates of IL-2 and IL-2RA mRNA production, respectively; f_1 and f_2 are the IL-2–dependent rates of IL-2 and IL-2RA mRNA production, respectively; $IL\text{-}2_p$ and $IL\text{-}2RA_P$ are the measured protein levels of IL-2 in the cell growth medium and surface IL-2Rα, respectively; and α denotes the degradation rate of each mRNA species (see below the parameter values that were used in the analysis). $K_{IL\text{-}2} + f_1(IL\text{-}2_P \times IL\text{-}2RA_P)$ and $K_{IL\text{-}2RA} + f2(IL\text{-}2_P \times IL\text{-}2RA_P)$ are the response functions of the two feedback loops, which we would like to extract. From equations 1 and 2, the response functions equal the sum of the time derivative at the left side and the degradation term on the right side. As we measured both mRNA species at high temporal resolution, it is possible to evaluate from data both mRNA level and its time derivative and obtain the shape of the response functions. mRNA levels of IL-2 and IL-2RA are normalized by the levels of a housekeeping gene (hypoxanthine phosphoribosyltransferase), hence, are less sensitive to changes in the number of cells during the experiment due to cell proliferation.

To relate the IL-2–dependent production terms (f_1, f_2) to the level of bound IL-2R, we estimate the latter as $IL\text{-}2_P \times IL\text{-}2RA_P$, that is, the level of IL-2 in the medium times the level of total IL-2Rα protein expressed by the cells. This is an approximation to the exact expression: $IL\text{-}2R_{bound} = C \times IL\text{-}2_{free} \times IL\text{-}12RA_{free}$. We measured $IL\text{-}2_{free}$ using ELISA. However, we cannot measure the level of free IL-2Rα because the available Abs do not distinguish between free and IL-2 bound receptors. Nevertheless, the approximation is reasonable for the IL-2R system. In particular, because the dissociation of IL-2 from IL-2Rα is fast, most IL-2Rα molecules are either free or bound in complexes containing the IL-2Rβ,γ subunits and IL-2 (10). Upon T cell activation, the number of IL-2Rα molecules per cell is much higher than that of the IL-2Rβ or γ subunits, and hence, most IL-2Rα is free, at least for CD25H cells. At earlier time points, total IL-2Rα might be an overestimation and levels of free IL-2Rα may actually be lower.

Because of technical constrains of the robotic system, we could not obtain ELISA measurements on the same cell cultures that were used for measuring mRNA and CD25 levels. Hence, we performed ELISA measurements on parallel cultures but at a lower time resolution. Because the changes in IL-2 protein levels in the cell culture medium are slower, we interpolated this data to estimate IL-2 levels at intermediate time points corresponding to the time resolution of the robotic measurements. We note that the main result of our model, regarding the relative levels of the thresholds of the two feedback loops, is robust to errors in the ELISA measurements and their interpolation—because these scale both response functions in a similar way.

Next, we fitted the data of Fig. 5 with Hill functions, to determine the parameters of the feedback response. We fitted IL-2RA production with a rising Hill function and IL-2 production with a declining Hill function: $ax^c/(x^c + b^c) + d$, using MATLAB. For a rising Hill, $c > 0$; for a declining Hill, $c < 0$. The resulting fits are displayed in Fig. 5. Fit has $R^2 = 0.98$ (0.79) for IL-2RA (IL-2). Fit parameters are given in Supplemental Table 1.

For the fit of the feedback on IL-2 production, we omitted the first four data points, which represent a delayed response in IL-2 mRNA levels following TCR activation. This delay may reflect the time needed for accumulation of IL-2 transcripts, which requires both TCR activation and stabilization of the IL-2 message mediated by CD28 costimulation.

mRNA degradation rates used for this calculation were 1.12 h^{-1} for IL-2 (15) and 0.4 h^{-1} for IL-2RA (16). In another study, a degradation rate for IL-2 mRNA was reported that differs by a factor of 2, using a different experimental system (17). Sensitivity analysis was performed on these rates resulting in no significant alteration of results for a 4-fold change. Specifically, the threshold value (value at half saturation) of the feedbacks,

b, changed by <20% over a 4-fold change in the values of mRNA degradation rates.

The Hill coefficient for the negative feedback on IL-2 cannot be constrained accurately with our data, because of the low number of data points at the transition region. The results are indicative of a sharp transition, but the exact value cannot be determined.

Results

IL-2Rα expression occurs in two discrete temporal phases

We studied the dynamics of the response of primary naive CD4$^+$ T cells from 5C.C7 TCR transgenic mice to a cognate peptide (MCC 88–103) presented by splenic DCs. The concentrations of peptide were varied over 4 orders of magnitude, and data were collected over 4 d. An initial examination of IL-2Rα levels suggested that expression was slow, appearing only at ∼40 h after addition of Ag, and increasing rapidly to 72 h, as reported previously (Fig. 1A) (10, 11, 18).

However, a careful examination of the expression of IL-2Rα during the first 24 h of culture revealed a more complex picture. Expression of IL-2Rα was undetectable on >99% of resting naive T cells (Fig. 1B, region N). This phenotype was maintained at all time points in the absence of Ag.

In the presence of Ag, an IL-2Rα positive population (CD25L cells) could rapidly be detected (Fig. 1B, region CD25L). The expression of IL-2Rα preceded any change in cell size, both as measured by FSC (Fig. 1B) and by flow microscopy (Fig. 1C, 1D). The level of IL-2Rα on CD25L cells was low, and IL-2Rα was expressed in distinct patches or microdomains on the cell surface (Fig. 1C, 1D). A patchy distribution is consistent with previous studies which reported that IL-2Rα was localized within membrane lipid rafts 20 h postactivation (19, 20), although the size of the patches appears rather large for conventional lipid rafts.

By day 2, IL-2Rα expression was qualitatively and quantitatively different, with cells either remaining small and IL-2Rα negative (naive) or appearing as larger cells with a significantly higher and more uniform IL-2Rα expression (CD25H cells, Fig. 1B, region CD25H; see also Fig. 1C, 1D).

Using the regions defined in Fig. 1B, we plotted the percentage of cells in each population as a function of both time and Ag level in Fig. 1E. Cells transition from naive to CD25L during the first day of culture at a rate determined by Ag concentration. Cells subsequently exit CD25L and enter CD25H. Over a wide range of Ag doses, the number of CD25H cells at 48 h is proportional to the number of CD25L at 19 h (Supplemental Fig. 1A), consistent with the hypothesis that CD25L cells are the precursors for CD25H cells. The maximum proportion of CD25L cells reached during the initial activation stage varied somewhat between experiments but was always <100%. The rapid fall in the percent of naive cells at later culture times (>40 h) was attributed to dilution by proliferating CD25H cells, as discussed in more detail below.

We repeated the experiment using other experimental models of T cell activation, including cells from OVA-specific OT-II transgenic mice (Supplemental Fig. 1B), and also with polyclonal CD4$^+$ T cells activated by anti-CD3 and anti-CD28 Abs. In both experimental setups, we observed cells with similar IL-2Rα expression kinetics and size profile as naive, CD25L, and CD25H, suggesting that the existence of these phases is a general feature of T cell activation.

The transition from naive to CD25L cells is Ag dependent and IL-2 independent and leads to rapid IL-2 secretion

Because the existence of two distinct phases of IL-2Rα expression has not been previously analyzed systematically, we investigated the characteristics of CD25L and CD25H cells in more detail. To attain high temporal resolution of the dynamics of the process, we used a robotic system in which cells were cultured and sampled for analysis at intervals of ∼3 h, over 3–4 d (see *Materials and Methods*). The level of CD25 expression began to increase by 6 h and then rose steadily (Fig. 2A). The rate of increase of CD25 (i.e., the slope of the mean fluorescence intensity (MFI) versus time) was Ag dose dependent. The proportion of cells within the CD25L gate (Fig. 2B) also began to increase from 6 h, with a rate that was dependent on Ag dose. At higher Ag concentrations, the maximum number of cells within the CD25L gate was reached by 12 h. Both these observations suggest that the rate of entry of cells from naive into the CD25L population increased with Ag dose. The level of IL-2RA mRNA rose rapidly at 6 h but then remained constant until the end of the first day of culture (Fig. 2C). The constant levels of IL-2RA mRNA (Fig 2C) and the constant rate of increase of surface IL-2Rα over this period (Fig. 2A) are consistent with a model in which IL-2Rα levels of CD25L cells are regulated mainly at the transcriptional level.

Production of IL-2 mRNA could be detected rapidly (Fig. 2D), peaking ∼10–15 h after activation, and then gradually declining. The transcriptional activity of the IL-2 gene was further followed at the single cell level using CD4 T cells from a homozygous IL2-GFP knockin 5C.C7 transgenic strain (21). These cells do not produce IL-2, but express GFP as a reporter for IL-2 promoter activity. During the first day of culture, GFP expression was found only in cells also expressing IL-2Rα (CD25L cells; Fig. 2E). At higher Ag concentrations (Fig. 2E, *left panel*), a greater proportion of cells entered CD25L, and a greater proportion expressed GFP, indicating activation of IL-2 transcription. Not all IL-2Rα–positive cells expressed GFP, consistent with previous reports (22). IL-2 levels in the cell growth medium, measured by ELISA, rose rapidly within the first day in an Ag-dependent way, reached a plateau and then remained constant or, at lower Ag concentrations, declined (Supplemental Fig. 1C).

Because IL-2Rα expression is known to be positively regulated via the IL-2R itself, we investigated whether IL-2Rα expression on CD25L cells was regulated by signaling via the IL-2R. We observed, however, that transition from naive to CD25L (shown by the proportion of cells within the CD25L gate) was not altered when using T cells from the IL-2 knockout (KO) (IL2-GFP knockin) mice (compare Fig. 2F, *first* and *second panels*), in which IL-2 secretion is absent. Adding back exogenous IL-2 to the IL-2 KO cultures at 0 h also did not alter the proportion of CD25L cells (Fig. 2F, *fourth panel*) or the amount of surface IL-2Rα per cell. Furthermore, a mixture of blocking Abs to IL-2, IL-2Rα, IL-2Rβ (CD122), and IL-15 strongly inhibited subsequent proliferation (Supplemental Fig. 2A) but did not influence either the rate of appearance of CD25L cells (Fig. 2F, *third panel*) or their IL-2Rα levels (Supplemental Fig. 2B, 2C). Thus, early IL-2Rα production is independent of signaling via the IL-2R.

In summary, CD25L cells are defined as a population of small T cells that express low levels of IL-2Rα and secrete IL-2. The transition from naive to CD25L cells is independent of IL-2 signaling but requires TCR signaling and its rate is a function of Ag dose.

The transition from CD25L to CD25H is dependent on IL-2 but not dependent on continued TCR signaling

CD25H cells started to appear at ∼1 d of culture. The levels of IL-2Rα per cell rose rapidly from around one day of culture and continued to rise until at least day 4 (Fig. 3A, *left panel*). Both the rate of rise of IL-2Rα and the final levels increased with Ag dose, although this saturated at the highest Ag dose tested. At the highest Ag concentration, IL-2Rα levels on CD25H cells are 20- to 40-fold higher than on CD25L cells. IL-2Rα mRNA also rose rapidly after the first day of culture (Supplemental Fig. 3A, 3B).

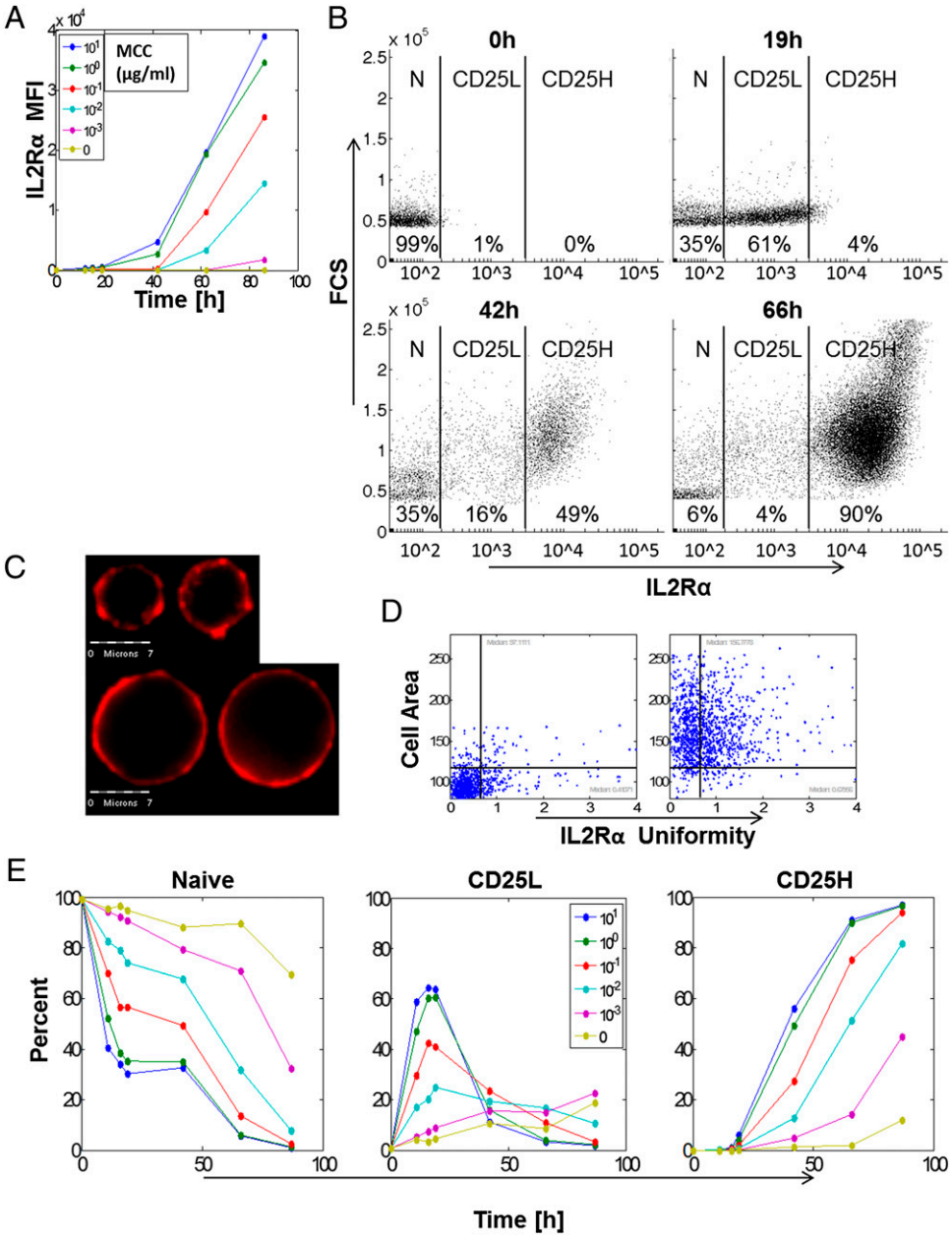

FIGURE 1. T cell activation occurs in two distinct phases. (**A**) Naive CD4$^+$ T cells were isolated from 5C.C7 TCR transgenic mice and incubated in the presence of C3H/HeJ DCs and 10 μg/ml (blue), 1 μg/ml (green), 0.1 μg/ml (red), 0.01 μg/ml (cyan), 0.001 μg/ml (magenta), or 0 μg/ml (yellow) MCC peptide. Cells were sampled over 87 h, and IL-2Rα (CD25) was detected by flow cytometry. IL-2Rα MFI of live CD4$^+$ T cells is plotted as a function of time. (**B**) Dot plots showing IL-2Rα and FSC of cells from the 1 μg/ml MCC group sampled at different times postactivation. (**C**) Cells activated with 1 μg /ml MCC were stained for IL-2Rα and analyzed using ImagestreamX flow microscopy. The figure shows images of typical cells sampled at either 15 h (*upper panel*) or 40 h (*lower panel*) postactivation. (**D**) Cell area and IL-2Rα distribution on cell membrane were quantified from flow microscopy images, as described in *Materials and Methods*. CD25L cells (*left panel*) showed smaller median cell area (97 μ^2), and lower median IL-2Rα uniformity (0.41 au) than CD25H cells (*right panel*, 157 μ^2 and 0.68 au, respectively). (**E**) The percentage of cells in the naive (*left panel*), CD25L (*middle panel*), and CD25H (*right panel*) populations as a function of time for the various Ag concentrations as in (**A**). N, No IL2Rα expression; CD25L, low IL2Rα expression; CD25H, high IL2Rα expression.

At the same time, levels of IL2 mRNA fell, continuously declining toward a very low level at ~68 h (Fig. 2D, Supplemental Fig. 3A, 3B). CD25H cells are therefore characterized by a large cell volume (Fig. 1C), very high IL-2Rα levels and rapidly declining IL-2 secretion.

We examined in more detail the factors that drive each of the above behaviors. In the absence of IL-2, using cells from the IL-2 KO (GFP-IL2 knockin) mice (Fig. 3A, *third panel*) or in the presence of Abs blocking IL-2 signaling (Fig. 3A, *second panel*), the upregulation of IL-2Rα (increased IL-2Rα MFI) on CD25H cells was strongly inhibited. Addition of exogenous IL-2 to the culture containing IL-2 KO cells restored high IL-2Rα expression (Fig. 3A, *fourth panel*). The switch to high IL-2Rα expression is therefore driven by the IL-2–IL-2R positive feedback loop.

We also noticed that the presence of exogenous IL-2 from the beginning of the cultures strongly repressed GFP expression in IL2-GFP knockin T cells (Fig. 3B). This observation is in agreement with previous reports describing a negative feedback of IL-2 on its own expression (14). Interestingly, however, high temporal resolution measurements (Fig. 3C) showed that the downregulation in

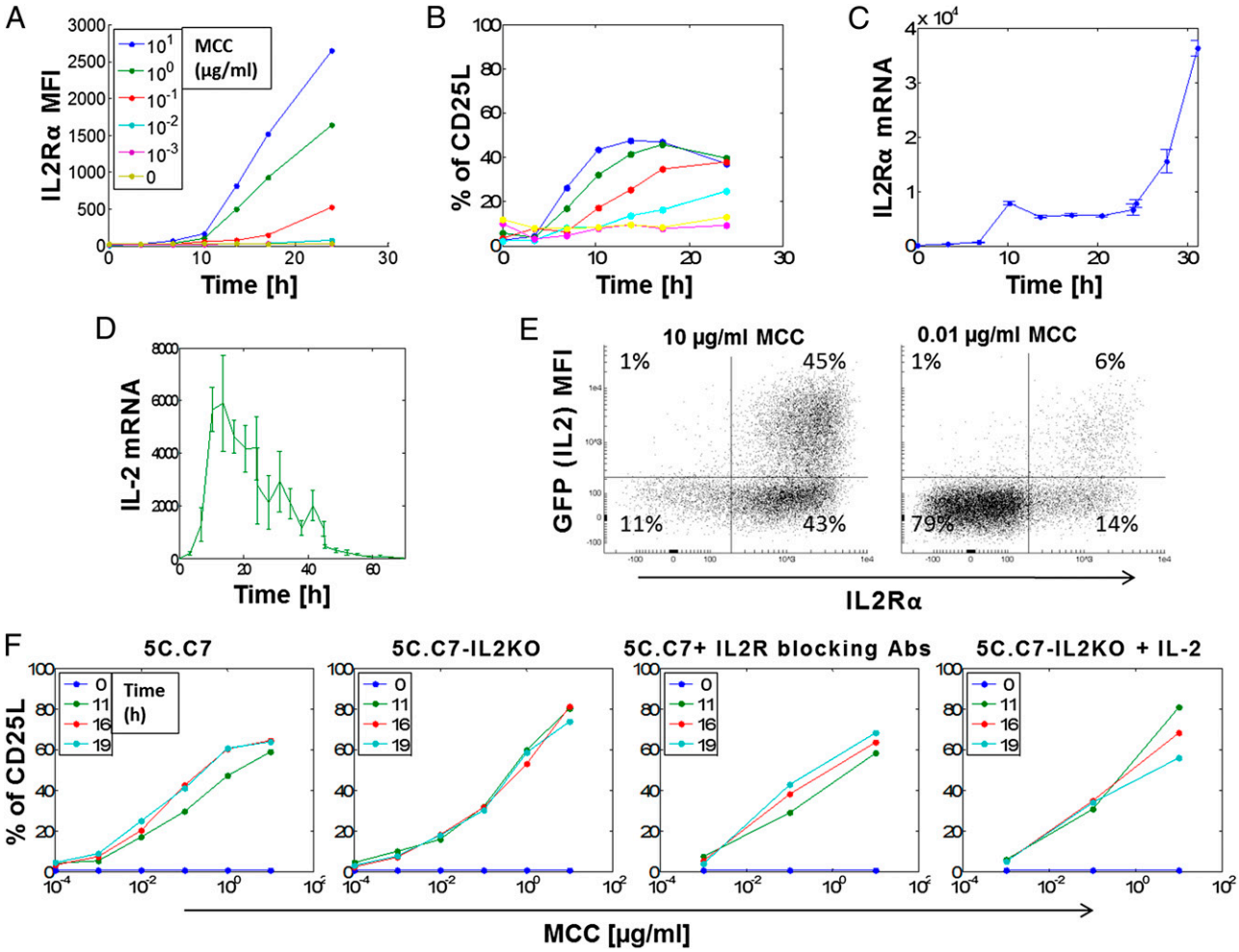

FIGURE 2. High temporal resolution analysis of the transition of naive cells to the CD25L phase demonstrates dependency on Ag but not IL-2. Naive $CD4^+$ T cells from 5C.C7 TCR transgenic mice were incubated in the presence of DCs and different levels of MCC peptide, as indicated. Cultures were sampled robotically every 3 h as described in *Materials and Methods*. IL-2Rα levels were measured by flow cytometry, using fluorescently labeled Abs. MFI of the total cell population (**A**) and the percentage of cells within the CD25L population (**B**) are shown as a function of time at different Ag concentrations. (**C**) RT-qPCR analysis of IL-2RA mRNA levels over the first 30 h of culture. Ag dose = 1 μg/ml MCC. Error bars represent SE of triplicates. (**D**) RT-qPCR analysis of IL-2 mRNA levels. Ag dose as in (C). (**E**) Naive $CD4^+$ T cells were isolated from 5C.C7 TCR transgenic mice, which express GFP from the IL-2 locus and are IL-2 deficient. Scatter plots of GFP versus IL-2Rα are shown for cells cultured for 19 h in the presence of 10 μg/ml (*left panel*) or 0.01 μg/ml (*right panel*) MCC. (**F**) The percentage of cells within the CD25L population as a function of peptide concentration at 0 h (blue), 11 h (green), 16 h (red), and 19 h (cyan) after activation. Similar behavior is observed for T cells isolated from 5C.C7 (*left panel*) and 5C.C7-IL2KO mice (*second panel*), although the latter do not express IL-2. Addition of saturating concentrations of blocking Abs against IL-2Rα, IL-2Rβ, IL-2, and IL-15 to 5C.C7 cells (*third panel*), or addition of 100 ng/ml IL-2 to 5C.C7-IL2KO cells (*fourth panel*) does not alter the percentage of cells entering the CD25L phase.

IL-2 transcriptional activity was only seen after 20 h, whereas at earlier time points, increased levels of the IL2-GFP reporter were not affected by external IL-2 (compare red and green lines in Fig. 3C during first 24 h). This observation is again suggestive of the lack of sensitivity to IL-2 during the first 20 h, when cells are mostly in CD25L.

Because both TCR and IL-2 signaling contribute to IL-2Rα levels, we set out to determine the role of Ag-dependent signals in driving the CD25L to CD25H transition. To dissociate the signal mediated via TCR signaling from that mediated via IL-2R signaling, we used CsA. CsA has been shown to have a variety of effects on cell signaling. However, CsA selectively blocks calceneurin-dependent signaling pathways, such as the NFAT-dependent TCR signaling pathway. In contrast, CsA does not block IL-2–mediated signaling, which does not involve calceneurin. CsA inhibited the rapid rise of IL-2Rα expression characteristic of CD25H cells if added at the start of cultures (green line in Fig. 3D) but not if added at 19 h of culture (red line in Fig. 3D). This result is consistent with a model in which TCR signaling via a CsA-sensitive pathway is required for naive to CD25L transition but is not required for the subsequent CD25L to CD25H transition, where IL-2 signaling is active.

CD25H cells proliferate, and their proliferation onset time and division rate are independent of Ag dose

An important output of the overall activation process is cell proliferation, which plays a key role in determining the number of effector and memory cells produced. We therefore investigated the relationship between proliferation (measured by dilution of CFSE) and the two phases of T cell activation that we described above.

No proliferation of CD25L cells was observed during our experiments (Fig. 4A, Supplemental Fig. 3C), although we cannot exclude that some late CD25L cells proliferated and differentiated into CD25H cells simultaneously. Therefore, although they expressed IL-2Rα at low levels and IL-2 is present in the culture medium, CD25L cells do not contribute significantly to the proliferation we observe. In contrast, proliferation of CD25H cells was seen, as demonstrated by

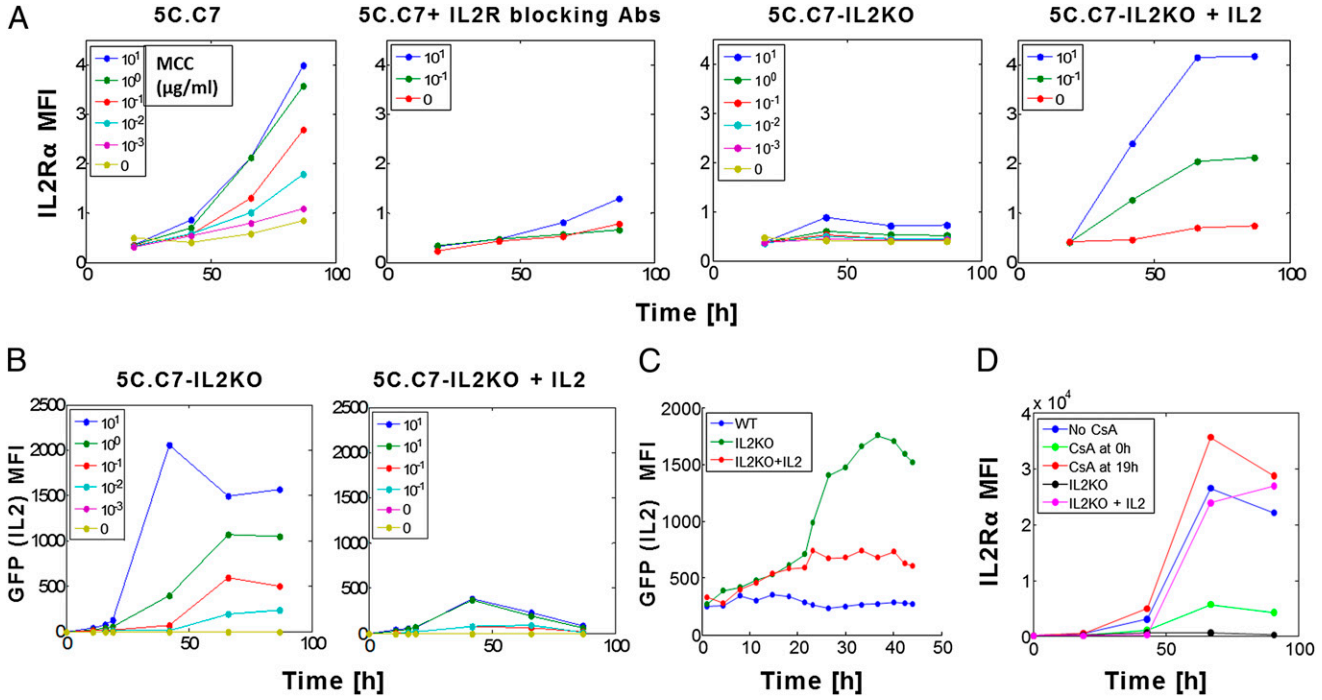

FIGURE 3. Entry into CD25H is regulated by IL-2 but does not require sustained TCR signaling. (**A**) MFI of IL-2Rα expression on CD25H cells, in the presence or absence of IL-2, as measured by flow cytometry. Naive $CD4^+$ T cells were isolated from 5C.C7 TCR transgenic mice or 5C.C7-IL2KO mice. MFI of IL-2Rα of the CD25H population is plotted as a function of time for different peptide concentrations. 5C.C7 cells were incubated with DCs and Ag as in previous figures, without (*left panel*) or with (*second panel*) saturating concentrations of Abs against IL-2Rα, IL-2Rβ, IL-2, and IL-15 added at time 0. 5C.C7-IL2KO cells were incubated without (*third panel*) or with (*fourth panel*) 100 ng/ml IL-2 added at time 0. (**B**) GFP expression of cells from 5C.C7-IL2KO mice, which express GFP from the IL-2 locus. Cells were cultured in the absence (*left panel*) or presence (*right panel*) of IL-2 (100 ng/ml), showing IL-2–mediated negative feedback on its expression level. (**C**) High temporal resolution measurement of GFP expression during the first 45 h after activation reveals that IL-2 negative feedback acts only after ~20 h, when most cells are in the CD25H phase. MCC concentration: 1 μg/ml. (**D**) MFI of IL-2Rα expression on cells incubated with DCs loaded with 1 μg/ml MCC in the presence or absence of 100 ng/ml CsA, added at either time 0 or 19 h post-activation. 5C.C7-IL2KO cells cultured with or without IL-2 (100 ng/ml) are shown for comparison.

dilution of CFSE staining in the cells with high CD25Rα MFI (Fig. 4A, *left panel*). Proliferation was first observed at ~34 h of culture consistent with previous studies (20). As expected, addition of CsA at the beginning of the culture blocked proliferation completely (Fig. 4A, *middle panel*), as did blocking of IL-2R by the Ab mixture (Supplemental Fig. 2A). However, CsA added after 19 h of culture had a negligible effect on proliferation (Fig. 4A, compare *far left* and *far right panels*), suggesting that once cells responded to Ag, further differentiation both in terms of IL-2Rα expression and proliferation was dependent on IL-2 but does not require sustained TCR signaling.

The number of cells after ~3 d of culture increased with Ag concentration (Fig. 4B, black, Supplemental Fig. 3D). Ag levels can affect eventual cell number by regulating either proliferation onset time (time to first division), proliferation rate following that first division, or the number of cells entering proliferation (23). To evaluate these possibilities, we followed cell numbers around the time of proliferation onset at high temporal resolution for the various Ag concentrations. We find that proliferation onset time and proliferation rate were Ag independent (Fig. 4C). This persisted even at 66 h, when number of cell divisions remained Ag independent (Fig. 4D). In contrast, the number of CD25H cells at the time of proliferation onset was dependent on Ag concentration (Fig. 4B, gray). On the basis of these results, we suggest that the level of Ag affects eventual cell number (or clone size) through varying the rate by which cells transfer from naive into the CD25L phase. At higher Ag levels, the increased transfer rate translates into a larger number of cells in CD25H at the onset of proliferation, which eventually results in a larger number of cells in the culture at later time points. We note that Ag levels may affect cell number also by changing the rate of cell death, which we did not address in this current analysis.

Extracting the response functions of IL-2 and IL-2RA from high temporal resolution data reveals coupled feedback loops

Previous studies have identified two feedback loops in the IL-2 system: a positive feedback driving IL-2RA expression (24) and a negative feedback regulating IL-2 expression (14, 25, 26). These feedbacks are characterized by their response function, namely the dependence of the promoter activity on the level of IL-2 signaling. Quantitative determination of these response functions is important for the modeling of the IL-2–IL-2R system, because they play crucial roles in shaping the system's response. However, the kinetic constants that characterize the response function of these feedback loops, such as their effective activation level and steepness, remain unknown. Estimating these parameters from measurements of protein levels is hampered by the fact that both IL-2 and IL-2R are consumed as a result of interaction between ligand and receptor. Estimating the response functions can be facilitated through measurements of mRNA levels, which, as we show below, are easier to interpret. Our analysis aims to relate the promoter activity of the IL-2RA and IL-2 genes to the level of IL-2R signaling. We use the fact that the promoter activity at any given time interval is equal to the net change in mRNA level plus the amount of mRNA that was degraded at this time interval (see *Materials and Methods* for details). In contrast, the response function mechanistically depends on the level of IL-2R signaling, which is a function of the levels of IL-2Rα on cell surface and IL-2 in the surrounding medium (*Materials and Methods*). Thus, our high temporal resolution mea-

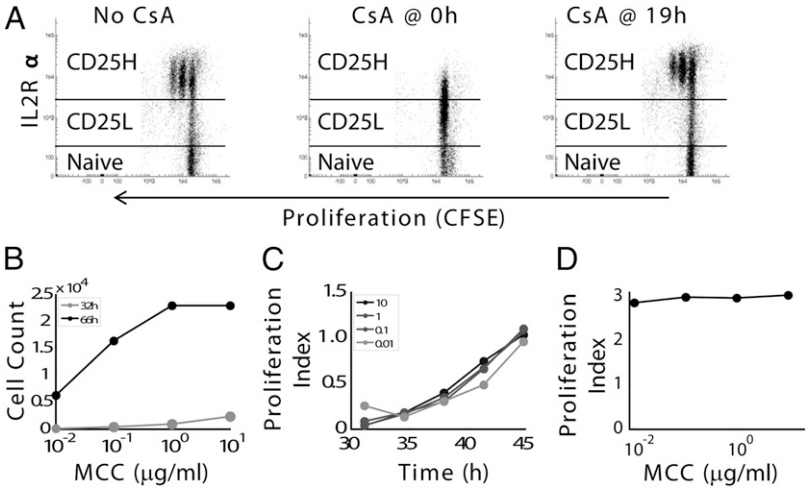

FIGURE 4. Characterization of cell proliferation. (**A**) Cell division is observed only for CD25H cells and does not require continuous TCR signaling. 5C.C7 T cells were stained with CFSE and incubated with DCs loaded with 1 μg/ml MCC peptide, without (*left panel*) or with CsA added either at 0 h (*middle panel*) or at 19 h (*right panel*). Shown are typical scatter plots of CD25 versus CFSE, measured 42 h after activation. (**B**–**D**) Dependence of final cell number on Ag concentration reflects differences in the number of cells entering CD25H phase but not in proliferation onset time or rate. 5C.C7 T cells were stained with CFSE and incubated with DCs loaded with 10, 1, 0.1, or 0.01 μg/ml MCC peptide. Cells were sampled at high temporal resolution around the time of the first division (30–45 h postactivation) and at an experimental endpoint (66 h). (B) The number of cells in CD25H as a function of peptide concentration is shown at proliferation onset (32 h, gray) and at 66 h (black). (C) Proliferation index (the population average number of divisions) is shown for different peptide concentrations for the time window around the first division. Proliferation onset time and proliferation rate are independent of peptide concentration. (D) Proliferation index of cells at 66 h is independent of peptide concentration.

surement of mRNA and protein levels allowed for direct estimation of the response functions of the two feedbacks.

Using this approach, we estimated the response functions by plotting the promoter activity of IL-2RA and IL-2 against an estimate for the level of IL-2 signaling (Fig. 5). The obtained data (points) were fitted using Hill functions (solid lines, see *Materials and Methods* for equations). Optimal fits gave very similar half saturation values for the two input functions (Supplemental Table 1). This finding indicates that positive feedback on IL-2RA and negative feedback on IL-2 occurred at similar levels of receptor occupancy, thus at a similar time point during the activation process (Fig. 6). The positive feedback on IL-2RA mRNA production is well fitted with a Hill coefficient of ~2. The negative feedback on IL-2 mRNA production, however, seems to have a much sharper response, although its exact slope could not be accurately determined from our data.

Discussion

Our investigation aimed to elucidate how Ag-specific signals combine with IL-2–mediated signals and IL-2–dependent regulatory feedback circuits to shape the overall process of naive T cell activation. The starting point for our investigation was a detailed kinetic analysis of IL-2Rα expression and IL-2 production. Robotic sampling at increased temporal resolution over several days revealed that the overall process could be divided into two distinct phases that we name CD25L and CD25H.

Several distinct pieces of evidence pointed to qualitative distinct phases. First, the levels of IL-2Rα during the first day of culture were much lower than those typically observed on activated T cells; IL-2Rα distribution in the cell membrane at these early times was patchy in accord with previous observations (19, 20); and its expression preceded any increase in cell volume typically accompanying full T cell activation.

Second, the existence of two discrete processes regulating IL-2Rα production also was indicated by their distinct Ag and IL-2 dependency. The appearance of CD25L cells within the first 20 h was dependent on TCR signaling but not on IL-2. This is supported by the fact that CsA, which blocks TCR signaling, completely blocked any IL-2Rα expression, whereas the rates of initial activation (transition into CD25L) and the levels of IL-2Rα expression on these cells were independent of IL-2 or IL-2R signaling. In contrast, the transition into the second phase of rapidly increasing IL-2Rα expression (CD25H, from ~24 h onward) was dependent on IL-2–mediated signaling but did not require continued TCR signaling. In addition, we observe proliferation only of CD25H cells and not CD25L cells. CsA blocks proliferation if added at the time of cell activation but fails to block it if added at 19 h when cells already have moved into CD25H. Thus, our data support a model of temporal segregation between pri-

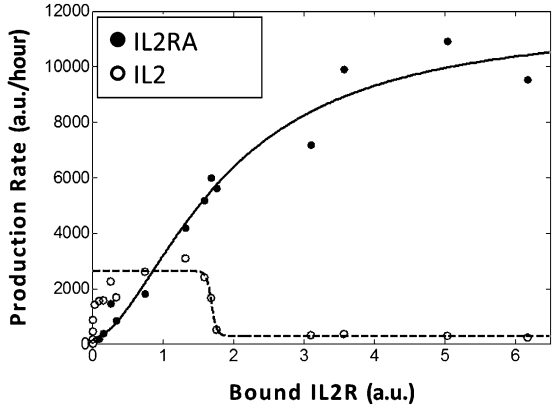

FIGURE 5. Extracting the response functions of IL-2 and IL-2RA feedback loops. The production rate of IL-2RA and IL-2 mRNA were plotted as function of an estimate for the level of receptor-bound IL-2, based on the high temporal resolution measurements of mRNA and proteins levels (see text for details). Data were fitted with a Hill function (see Supplemental Table 1 for fitting parameters). The two response functions have a similar threshold level (~1.8 au) but have different sensitivity at threshold (different slopes).

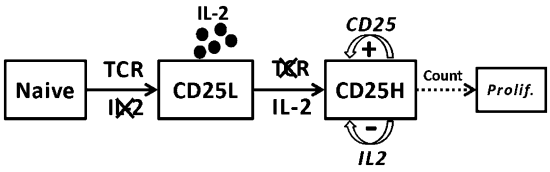

FIGURE 6. A schematic model describing the observed two-phase behavior and its dependencies. Transition of naive cells into CD25L is driven by TCR and is independent of IL-2–mediated signaling. CD25L cells secrete IL-2, express low levels of CD25, and do not proliferate. Transition from CD25L to CD25H depends on sufficient IL-2–mediated signaling but does not require continued TCR signaling. CD25 expression is augmented, and IL-2 expression is reduced by their corresponding extracellular positive and negative feedbacks, both driven by IL-2. The cells that are in CD25H can proliferate.

vate signals (i.e., Ag and costimulation) and public, shared signals (soluble cytokines) driving T cell activation (Fig. 6). Only when licensed by the first, private signal do cells become sensitive to the public one.

Third, the pattern of IL-2 production was also distinct in CD25L and CD25H cells. We tracked IL-2 production by RT-qPCR of message (Fig. 2D) by the ELISA of secreted protein (Supplemental Fig. 1C) and by measuring the expression of a GFP reporter transgene integrated into the IL-2 locus (Fig. 3C). The combination of these three measurements suggested there was rapid IL-2 production accompanying the initial transition from naive to activated cells, which continued throughout the CD25L phase. Subsequently, IL-2 transcription and protein production were switched off, consistent with a negative feedback loop as described previously (14, 25, 26). We find that the negative feedback of IL-2 signaling on IL-2 production is not active during the first phase, and only becomes effective for CD25H cells. The consequences of these two processes was that after ~2 d in culture, because IL-2 production stopped and IL-2Rα levels rose, net IL-2 concentrations leveled off or fell because of its consumption by the cells.

These findings promoted us to investigate the mechanism that establishes the two distinct phases, focusing on the IL-2–mediated positive feedback on IL-2RA and negative feedback on IL-2. We demonstrate a new method for extracting quantitative parameters of these feedbacks, using high temporal resolution data of both mRNA and protein levels. This method can be used to evaluate response functions of other cytokine-mediated extracellular feedbacks, such as IL-4 (27). A limitation of our approach is that it uses average values for expression of the various molecular components, thus ignoring the heterogeneity and stochastic elements of the system. Coupling of nonlinear feedback circuits acting between heterogeneous populations of cells might generate interesting and unexpected outcomes, and further studies, using single-cell measurements of each component, would therefore be very valuable. For the IL-2 system, we find that the two feedbacks are coupled, namely they have similar half-saturation values. As a result, the negative and positive feedback loops become active at similar levels of IL-2R signaling, hence, at a similar time during the activation process. This coupling between the feedbacks may be a result of their dependence on the same signal mediated by IL-2–IL-2R, although they also may be actively coupled through an unknown direct regulatory mechanism. In contrast, the Hill coefficients of the two feedbacks (i.e., steepness of feedback response at half-saturation) seem different, implying distinct intracellular mechanisms. Indeed, although positive feedback on IL-2RA is likely mediated directly via STAT5 binding to the IL-2RA promoter (24), negative feedback on IL-2 is likely to involve complex interactions between transcription factors building a repressor complex (26). Another intriguing possibility is that the sharp shutoff of IL-2 is reflecting regulation of IL-2 mRNA via micro-RNA–mediated degradation. It was shown that such regulation can result in sharper transitions than typically offered by transcription factor regulation (28–30). Recently, miRNA had been shown to modulate IL-2 production (31). It will be interesting to check if this regulation can mediate a sharp shutoff of IL-2 in response to IL-2 signaling.

The existence of two opposing coupled feedback loops can explain the observed two-phase behavior. Naive T cells do not express IL-2 and IL-2Rα at significant levels. Upon Ag stimulations, cells start making both proteins. However, because both feedback loops depend on IL-2R signaling, they are not functional at first; even though IL-2 is produced and can accumulate in the cells' environment, levels of receptor are low, and cells remain unresponsive to IL-2. Thus, cells are locked in the CD25L phase in which IL-2 is produced at a high rate (negative feedback is not active), and IL-2Rα is produced at a low rate (positive feedback is not active). Only when receptor levels reach a threshold level both feedbacks become active. This results in transition of the cells into the CD25H phase in which IL-2 production is turned off (negative feedback is active), whereas IL-2Rα production rate is highly increased (positive feedback is active).

We conclude by speculating briefly on the possible biological significance of the two-phase model of CD4 T cell activation. We suggest that CD25L and CD25H cells can be considered as "producers" and "consumers" of IL-2, respectively. CD25L cells produce maximal levels of IL-2 but cannot consume much IL-2 because their receptor level is low. However, as IL-2 and IL-2Rα both increase, cells switch to consumer status. IL-2 production then falls (via negative feedback), and at the same, time IL2 consumption grows as IL-2Rα levels rise. The nature of our analysis dictated an in vitro investigation. However, we suggest that our observation of two phases of activation in vitro can be related to observations on the dynamic behavior of T cells within lymph nodes following Ag-mediated activation. Two photon microscopy studies on intact lymph nodes have demonstrated that T cells sample DCs for a few hours, serially engaging their TCR (32). Following this first stage, clusters of T cells arrest on a DC for several hours, forming long lasting contacts while secreting IL-2 and potentially other cytokines (33). We suggest that T cell arrest and clustering may serve not only for communication with the DC but rather to maintain a microenvironment enriched with cells that already have sensed a sufficient level of the private signal and are now interacting via shared signals to reach a communal decision driving further proliferation and differentiation. Intercellular interactions mediated by IL-2 during this stage can lead to cooperation or competition between effector T cells (34) and to inhibition of effector T cells by Treg cells (10, 11). The importance of such shared signals within the microenvironment of an in vivo DC/T cell cluster, where both Ag-specific T cells and Ag-bearing DCs are rare and where gradients of cytokines are likely to be very sharp, might in fact be much greater than in the context of the in vitro transgenic model explored in this study.

Finally, CD25H cells, with high IL-2Rα, little or no IL2 production and increased CTLA-4 levels (Supplemental Fig. 3E), are reminiscent of Treg cells. Thus, these cells may regulate ongoing T cell responses by cell–cell contact and also through IL-2 consumption (10, 11). Proliferation, which rapidly produces large numbers of CD25H cells, further contributes to the negative regulation. Therefore, we posit that the two-phase behavior of the IL-2/IL-2RA system during CD4 Ag-driven activation is self-regulating and can act in concert with Treg cells to limit the magnitude of the resulting immune response in time and space.

Disclosures

The authors have no financial conflicts of interest.

References

1. Chakraborty, A. K., and J. Das. 2010. Pairing computation with experimentation: a powerful coupling for understanding T cell signalling. *Nat. Rev. Immunol.* 10: 59–71.
2. Hasbold, J., A. V. Gett, J. S. Rush, E. Deenick, D. Avery, J. Jun, and P. D. Hodgkin. 1999. Quantitative analysis of lymphocyte differentiation and proliferation in vitro using carboxyfluorescein diacetate succinimidyl ester. *Immunol. Cell Biol.* 77: 516–522.
3. Davis, M. M., M. Krogsgaard, J. B. Huppa, C. Sumen, M. A. Purbhoo, D. J. Irvine, L. C. Wu, and L. Ehrlich. 2003. Dynamics of cell surface molecules during T cell recognition. *Annu. Rev. Biochem.* 72: 717–742.
4. Huse, M., L. O. Klein, A. T. Girvin, J. M. Faraj, Q.-J. Li, M. S. Kuhns, and M. M. Davis. 2007. Spatial and temporal dynamics of T cell receptor signaling with a photoactivatable agonist. *Immunity* 27: 76–88.
5. Meuer, S. C., R. E. Hussey. D. A. Cantrell, J. C. Hodgdon, S. F. Schlossman, K. A. Smith, and E. L. Reinherz. 1984. Triggering of the T3-Ti antigen-receptor complex results in clonal T-cell proliferation through an interleukin 2-dependent autocrine pathway. *Proc. Natl. Acad. Sci. USA* 81: 1509–1513.
6. Horak, I., J. Löhler, A. Ma, and K. A. Smith. 1995. Interleukin-2 deficient mice: a new model to study autoimmunity and self-tolerance. *Immunol. Rev.* 148: 35–44.
7. Burchill, M. A., J. Yang, C. Vogtenhuber, B. R. Blazar, and M. A. Farrar. 2007. IL-2 receptor β-dependent STAT5 activation is required for the development of $Foxp3^+$ regulatory T cells. *J. Immunol.* 178: 280–290.
8. D'Cruz, L. M., and L. Klein. 2005. Development and function of agonist-induced $CD25^+Foxp3^+$ regulatory T cells in the absence of interleukin 2 signaling. *Nat. Immunol.* 6: 1152–1159.
9. Smith, K. A. 1988. The interleukin 2 receptor. *Adv. Immunol.* 42: 165–179.
10. Feinerman, O., G. Jentsch, K. E. Tkach, J. W. Coward, M. M. Hathorn, M. W. Sneddon, T. Emonet, K. A. Smith, and G. Altan-Bonnet. 2010. Single-cell quantification of IL-2 response by effector and regulatory T cells reveals critical plasticity in immune response. *Mol. Syst. Biol.* 6: 437.
11. Busse, D., M. de la Rosa, K. Hobiger, K. Thurley, M. Flossdorf, A. Scheffold, and T. Höfer. 2010. Competing feedback loops shape IL-2 signaling between helper and regulatory T lymphocytes in cellular microenvironments. *Proc. Natl. Acad. Sci. USA* 107: 3058–3063.
12. Waldmann, T. A. 1989. The multi-subunit interleukin-2 receptor. *Annu. Rev. Biochem.* 58: 875–911.
13. Meyer, W. K., P. Reichenbach, U. Schindler, E. Soldaini, and M. Nabholz. 1997. Interaction of STAT5 dimers on two low affinity binding sites mediates interleukin 2 (IL-2) stimulation of IL-2 receptor α gene transcription. *J. Biol. Chem.* 272: 31821–31828.
14. Villarino, A. V., C. M. Tato, J. S. Stumhofer, Z. Yao, Y. K. Cui, L. Hennighausen, J. J. O'Shea, and C. A. Hunter. 2007. Helper T cell IL-2 production is limited by negative feedback and STAT-dependent cytokine signals. *J. Exp. Med.* 204: 65–71.
15. Shi, L., W. R. Godfrey, J. Lin, G. Zhao, and P. N. Kao. 2007. NF90 regulates inducible IL-2 gene expression in T cells. *J. Exp. Med.* 204: 971–977.
16. Cerdan, C., Y. Martin, M. Courcoul, H. Brailly, C. Mawas, F. Birg, and D. Olive. 1992. Receptor α/CD25 expression after T cell activation via the adhesion molecules CD2 and CD28. *J. Immunol.* 149: 2255–2261.
17. Umlauf, S. W., B. Beverly, O. Lantz, and R. H. Schwartz. 1995. Regulation of interleukin 2 gene expression by CD28 costimulation in mouse T-cell clones: both nuclear and cytoplasmic RNAs are regulated with complex kinetics. *Mol. Cell. Biol.* 15: 3197–3205.
18. Kim, H. P., J. Imbert, and W. J. Leonard. 2006. Both integrated and differential regulation of components of the IL-2/IL-2 receptor system. *Cytokine Growth Factor Rev.* 17: 349–366.
19. Marmor, M. D., and M. Julius. 2001. Role for lipid rafts in regulating interleukin-2 receptor signaling. *Blood* 98: 1489–1497.
20. Lamaze, C., A. Dujeancourt, T. Baba, C. G. Lo, A. Benmerah, and A. Dautry-Varsat. 2001. Interleukin 2 receptors and detergent-resistant membrane domains define a clathrin-independent endocytic pathway. *Mol. Cell* 7: 661–671.
21. Naramura, M., R. J. Hu, and H. Gu. 1998. Mice with a fluorescent marker for interleukin 2 gene activation. *Immunity* 9: 209–216.
22. Sojka, D. K., D. Bruniquel, R. H. Schwartz, and N. J. Singh. 2004. IL-2 secretion by $CD4^+$ T cells in vivo is rapid, transient, and influenced by TCR-specific competition. *J. Immunol.* 172: 6136–6143.
23. Deenick, E. K., A. V. Gett, and P. D. Hodgkin. 2003. Stochastic model of T cell proliferation: a calculus revealing IL-2 regulation of precursor frequencies, cell cycle time, and survival. *J. Immunol.* 170: 4963–4972.
24. Kim, H. P., J. Kelly, and W. J. Leonard. 2001. The basis for IL-2-induced IL-2 receptor α chain gene regulation: importance of two widely separated IL-2 response elements. *Immunity* 15: 159–172.
25. Martins, G., and K. Calame. 2008. Regulation and functions of Blimp-1 in T and B lymphocytes. *Annu. Rev. Immunol.* 26: 133–169.
26. Gong, D., and T. R. Malek. 2007. Cytokine-dependent Blimp-1 expression in activated T cells inhibits IL-2 production. *J. Immunol.* 178: 242–252.
27. Renz, H., J. Domenico, and E. W. Gelfand. 1991. IL-4-dependent up-regulation of IL-4 receptor expression in murine T and B cells. *J. Immunol.* 146: 3049–3055.
28. Inui, M., G. Martello, and S. Piccolo. 2010. MicroRNA control of signal transduction. *Nat. Rev. Mol. Cell Biol.* 11: 252–263.
29. Levine, E., Z. Zhang, T. Kuhlman, and T. Hwa. 2007. Quantitative characteristics of gene regulation by small RNA. *PLoS Biol.* 5: e229.
30. Mehta, P., S. Goyal, and N. S. Wingreen. 2008. A quantitative comparison of sRNA-based and protein-based gene regulation. *Mol. Syst. Biol.* 4: 221.
31. Curtale, G., F. Citarella, C. Carissimi, M. Goldoni, N. Carucci, V. Fulci, D. Franceschini, F. Meloni, V. Barnaba, and G. Macino. 2010. An emerging player in the adaptive immune response: microRNA-146a is a modulator of IL-2 expression and activation-induced cell death in T lymphocytes. *Blood* 115: 265–273.
32. Mempel, T. R., S. E. Henrickson, and U. H. Von Andrian. 2004. T-cell priming by dendritic cells in lymph nodes occurs in three distinct phases. *Nature* 427: 154–159.
33. Henrickson, S. E., T. R. Mempel, I. B. Mazo, B. Liu, M. N. Artyomov, H. Zheng, A. Peixoto, M. P. Flynn, B. Senman, T. Junt, et al. 2008. T cell sensing of antigen dose governs interactive behavior with dendritic cells and sets a threshold for T cell activation. *Nat. Immunol.* 9: 282–291.
34. Savir, Y., N. Waysbort, Y. E. Antebi, T. Tlusty, and N. Friedman. 2012. Balancing speed and accuracy of polyclonal T cell activation: a role for extracellular feedback. *BMC Syst. Biol.* 6: 111.